Supplementary Data for

AIBP protects retinal ganglion cells against neuroinflammation and mitochondrial dysfunction in glaucomatous neurodegeneration

Soo-Ho Choi[a,*†], Keun-Young Kim[b*], Guy A. Perkins[b], Sébastien Phan[b], Genea Edwards[c‡], Yining Xia[a], Jungsu Kim[a], Dorota Skowronska-Krawczyk[d], Robert N. Weinreb[c], Mark H. Ellisman[b], Yury I. Miller[a,§] and Won-Kyu Ju[c,†,§]

[†]Co-corresponding authors: Dr. Won-Kyu Ju and Dr. Soo-Ho Choi
Email: wju@health.ucsd.edu
Email: soc002@health.ucsd.edu

This PDF file includes:

Graphic Abstract Legend
Supplemental Figures 1 to 4
Supplemental Tables 1 and 2
Supplemental Movie Legends 1 to 6

Other supplementary materials for this manuscript include the following:

Supplemental Movies 1 to 6

Graphic Abstract Legend.

Hypothetical models for protective roles of AIBP against neuroinflammation and mitochondrial dysfunction in glaucomatous neurodegeneration. Normal function of AIBP in resident Müller glia and RGC survival. Mitochondrial dysfunction and neuroinflammation in *Apoa1bp*$^{-/-}$ Müller glia and their effect on RGC loss and visual dysfunction. Elevated IOP-induced glial activation, mitochondrial dysfunction, neuroinflammation and RGC death. AIBP could be a potential therapeutic agent by blocking TLR4 signaling, mitochondrial dysfunction and neuroinflammation in glaucomatous neurodegeneration.

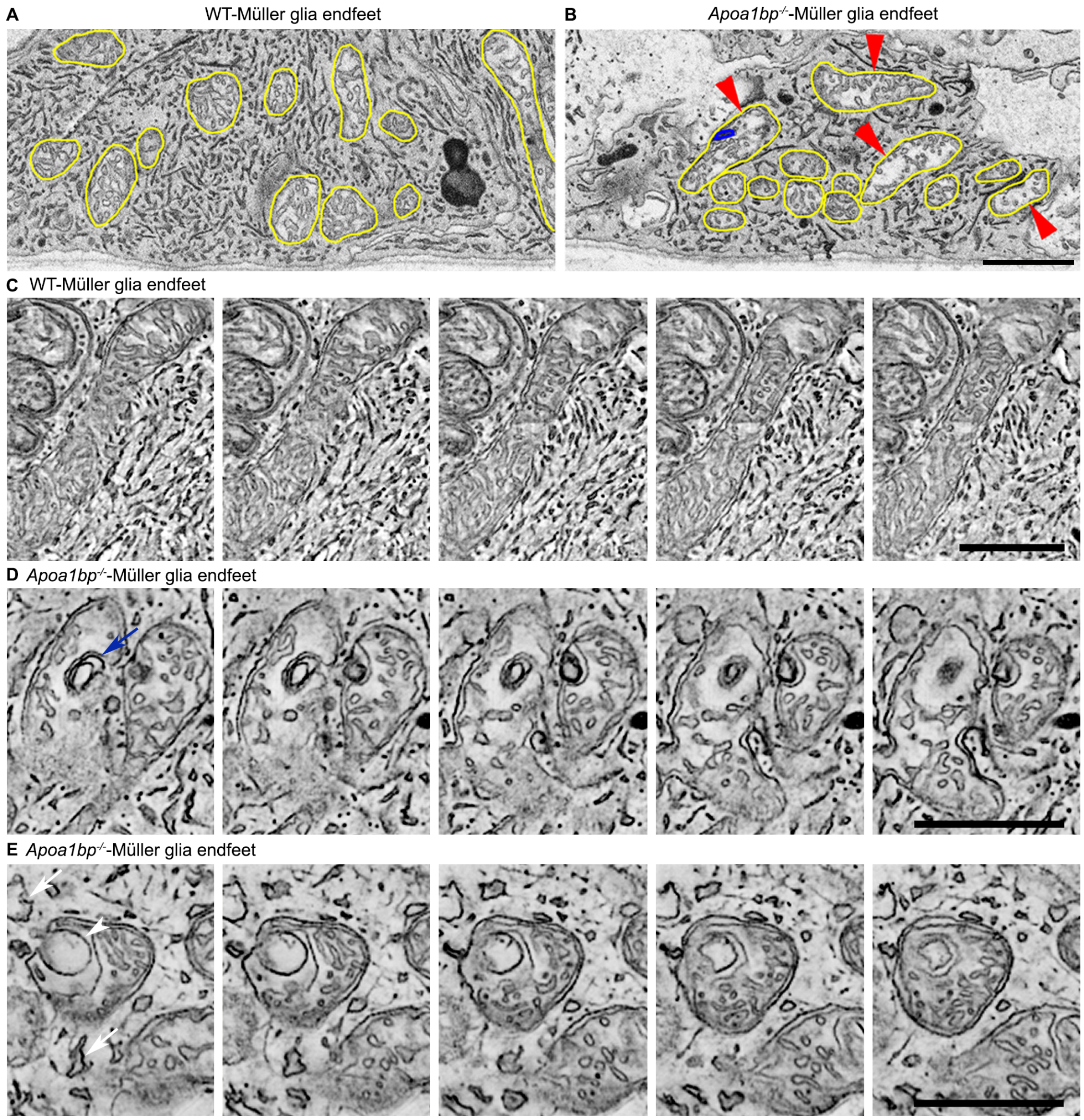

Supplementary Figure 1. AIBP deficiency induces abnormal structures of mitochondria and rough ER, and mitophagosome formation in Müller glia endfeet. (*A*) Color added to an additional slice to highlight the WT mitochondria (yellow trace). (*B*) Color added to an additional slice to not only identify the mitochondria (yellow trace), but also to point to the mitochondria with lower cristae density (red arrowheads) compared to the WT traced and a dark outer membrane onion-like swirl (blue trace). (*C-E*) Serial slice images through the tomographic volume from WT and *Apoa1bp*$^{-/-}$ Müller glia endfeets. (*C*) Serial slice images from WT Müller glia endfeet showing a long tubular form of mitochondrion with abundant rough ER. (*D*) Serial slice images from *Apoa1bp*$^{-/-}$ Müller glia endfeet to point to the mitochondria with lower cristae density and dark outer membrane onion-like swirls (blue arrow). (*E*) Serial slice images from *Apoa1bp*$^{-/-}$ Müller glia endfeet an abnormal mitochondrion with a vesicular inclusion (arrowhead) as well as lower rough ER density and dilated rough ER strands (arrows). Scale bars: 1 μm (*A-D*).

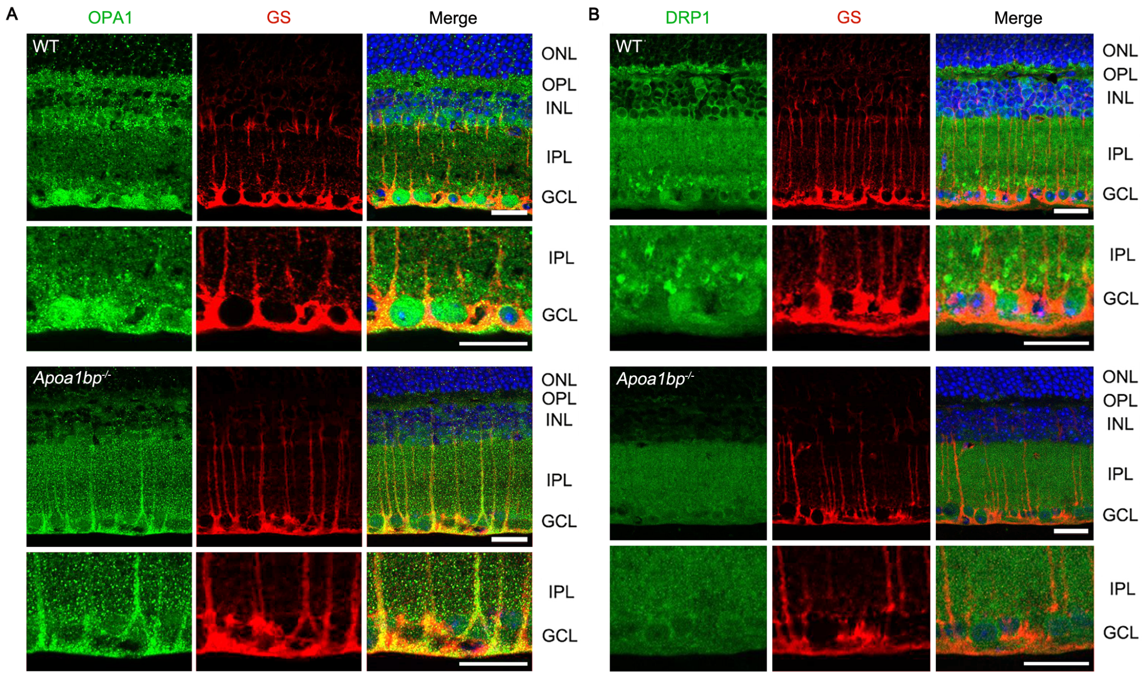

Supplementary Figure 2. AIBP deficiency impairs mitochondrial dynamics and OXPHOS activity in the retina. (*A*) Representative images from immunohistochemical analyses showed OPA1 (green) and GS (red) immunoreactivities in the wax sections from WT and *Apoa1bp*$^{-/-}$ retinas. Note that OPA1 immunoreactivity was decreased in the inner retinal layer but increases in Müller glia of *Apoa1bp*$^{-/-}$ retina. (*B*) Representative images from immunohistochemical analyses showed DRP1 (green) and GS (red) immunoreactivities in the wax sections from WT and *Apoa1bp*$^{-/-}$ retinas. Note that DRP1 immunoreactivity was decreased in the inner retinal layer but did not detected in Müller glia of *Apoa1bp*$^{-/-}$ retina. Blue is Hoechst 33342 staining for nucleus. Scale bar: 20 µm. GCL, ganglion cell layer; INL, inner nuclear layer; IPL, inner plexiform layer; ONL, outer nuclear layer; OPL, outer plexiform layer.

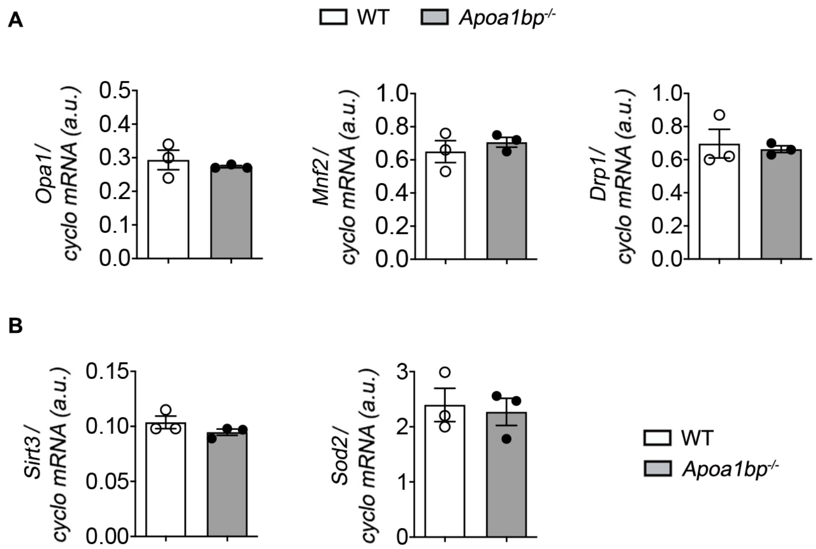

Supplementary Figure 3. AIBP deficiency does not affect mitochondrial dynamics- and oxidative stress-related gene expression in the retina. (*A* and *B*) *Opa1, Nfn2,* and *Drp1, as well as Sirt3 and Sod2* gene expression was assessed by quantitative PCR analysis in WT and *Apoa1bp*$^{-/-}$ retinas. Note that there were no statistically significant differences in *Opa1, Mfn2,* and *Drp1* (*A*), *as well as Sirt3 and Sod2* (*B*) gene expression. *n* = 3 mice. Error bars represent SEM.

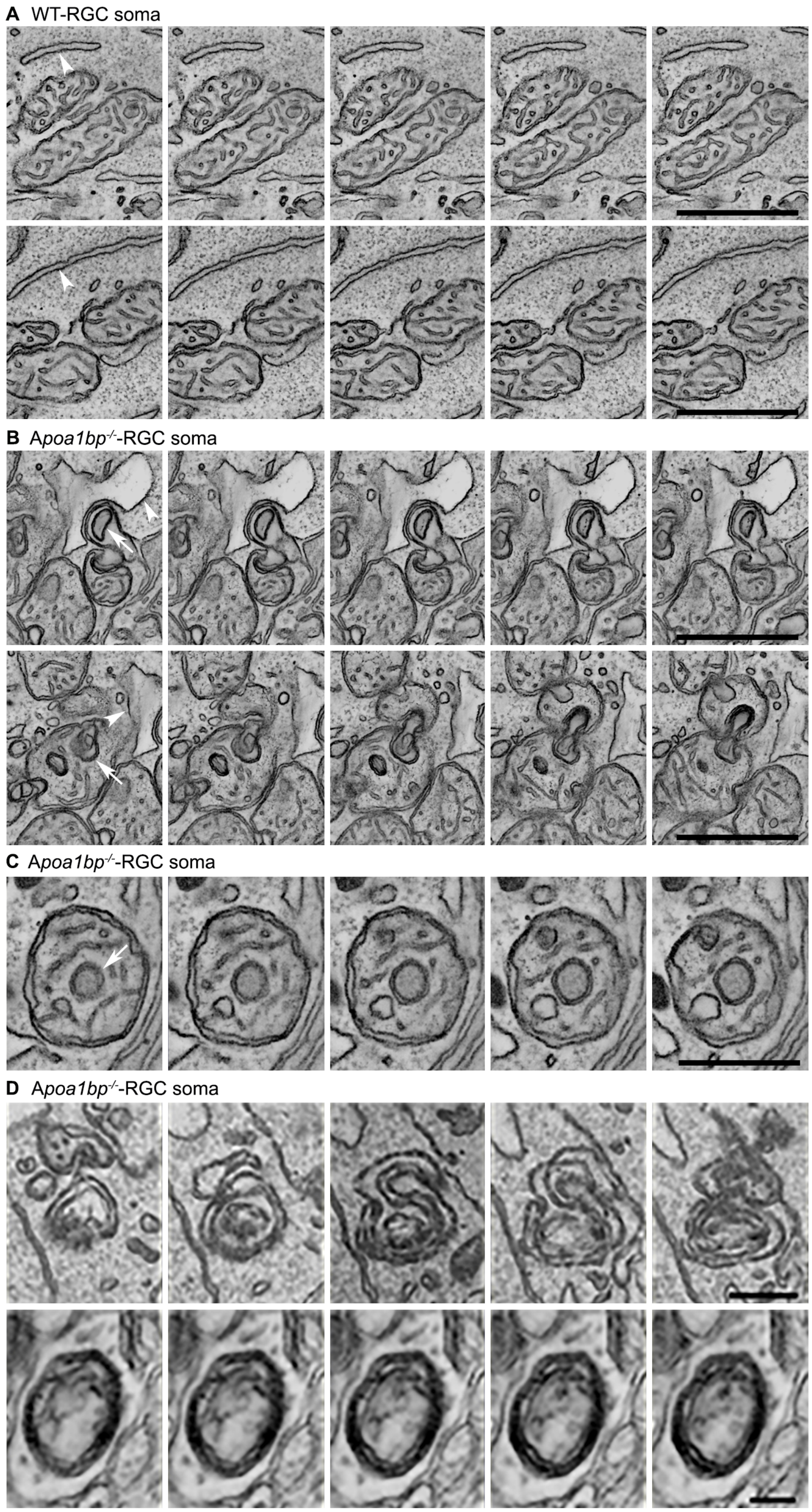

Supplementary Figure 4. AIBP deficiency induces abnormal structure of mitochondria and ER, and mitophagosome formation in RGC soma. (*A-D*) Serial slice images through the tomographic volume from WT and *Apoa1bp*$^{-/-}$ RGC somas. (*A*) Serial slice images from WT Müller glia endfeet showing a long tubular form of mitochondria with normal structure of ER strands (arrowheads). (*B*) Serial slice images from *Apoa1bp*$^{-/-}$ RGC soma to point to the dark outer membrane onion-like swirls (arrows) and dilated ER strands (arrowheads). (*C*) Serial slice images from *Apoa1bp*$^{-/-}$ RGC soma showing a ring-shaped mitochondrion (arrow). (*D*) Serial slice images from *Apoa1bp*$^{-/-}$ RGC soma showing two ongoing autophagosome formation. Scale bars: 1 μm (*A-D*).

Supplementary Table 1. List of Antibodies

Target antigen	Vendor or Source	Catalog No	Working concentration
ABCA1	Novus Biologicals	NB400-105	1:100 (IF)
AIBP	Novus Biologicals	NBP2-30626	1:100 (IF)
AIBP (Rabbit polyclonal)	Kind gift from Dr. Longhou Fang	N/A	1:5000 (WB)
BRN3A	Santa Cruz Biotechnology	sc-31894	1:200 (IF)
Cytochrome C	Zymed	33-8500	1:100 (IF)
DRP1	Santa Cruz Biotechnology	sc-32898	1:1000 (WB) 1:50 (IF)
ERK1/2	Cell Signaling Technology	1240	1:1000 (WB)
Glutamine Synthase (GS)	Proteintech	11037-2-1P	1:300 (IF)
Glutamine Synthase (GS)	Chemicon	MAB302	1:300 (IF)
Goat anti-rabbit HRP	Cell Signaling Technology	7074	1:3000 (WB)
Goat anti-mouse HRP	Cell Signaling Technology	7076	1:3000 (WB)
IL-1β	Abcam	ab9722	1:100 (IF)
MFN2	Cell Signaling Technology	9482	1:1000 (WB)
OPA1	BD Biosciences	612607	1:1000 (WB) 1:100 (IF)
OXPHOS	Invitrogen	45-7999	1:5000 (WB)
p38	Cell Signaling Technology	8690	1:1000 (WB)
Phospho-p38	Cell Signaling Technology	4511	1:1000 (WB) 1:100 (IF)
p65	Cell Signaling Technology	8242	1:1000 (WB)
Phospho-p65	Cell Signaling Technology	3033	1:1000 (WB)
Phospho-DRP1 S637	Cell Signaling Technology	6319	1:1000 (WB)
Phospho-ERK1/2	Cell Signaling Technology	4370	1:1000 (WB) 1:100 (IF)
RBPMS	Novus Biologicals	NBP2-20112	1:300 (IF)
SIRT3	Cell Signaling Technology	5490	1:1000 (WB) 1:100 (IF)
SOD2	Santa Cruz Biotechnology	sc-30080	1:1000 (WB) 1:300 (IF)
TLR4	Proteintech	19811-1-AP	TLR4 (IF)
TUJ1	BioLegend	801202	1:300 (IF)
VDAC	Cell Signaling Technology	4661	1:1000 (WB)
β-ACTIN	Cell Signaling Technology	4967	1:1000 (WB)
Alexa Fluor-488 conjugated donkey anti-mouse IgG antibody	Invitrogen	A-21203	1:100 (IF)
Alexa Fluor-488 conjugated donkey anti-rabbit IgG antibody	Invitrogen	A-21206	1:100 (IF)

Alexa Fluor-568 conjugated donkey anti-mouse IgG antibody	Invitrogen	A-10042	1:100 (IF)
Alexa Fluor-568 conjugated donkey anti-goat IgG antibody	Invitrogen	A-11057	1:100 (IF)
Alexa Fluor-649 conjugated donkey anti-goat IgG antibody	Invitrogen	A-21447	1:100 (IF)

WB, Western blot; IF, Immunofluorscence

Supplementary Table 2. List of Primers

Target gene	Primers
Mouse *Apoa1bp*	GACGAGCTGTATGAGCTGGTGG (F)
	CTGTAGACGGTAGACACACTCTG (R)
Mouse *Cyclo (Cyclophilin A)*	TGGAGAGCACCAAGACAGACA (F)
	TGCCGGAGTCGACAATGAT (R
Mouse *Drp1*	GCGCAGAACTCTAGCTGTAAT (F)
	CTGGAATAACCCTTCCCATCAA (R)
Mouse *Mfn2*	CAAGACCGGCTGAGGTTTATT (F)
	CCTTTCCACTTCCTCCGTAATC (R)
Mouse *Mitofilin*	GCCCAATGTCACTCACTACT (F)
	CCCGTCGATGTTCTGTGTATAG (R)
Mouse *Opa1*	CTCCCGACTTGGACAAGATTAC (F)
	CCATGATCTGTTGCTCGAAATG (R)
Mouse *Sirt3*	GCCCAATGTCACTCACTACTT (F)
	CCCGTCGATGTTCTGTGTATAG (R)
Mouse *Sod2*	AGCGTGACTTTGGGTCTTT (F)
	AGCGACCTTGCTCCTTATTG (R)

Supplemental Movie Legend

Supplemental Movie 1. Rotating view of the final 3D images of WT Müller glia mitochondria. Surface rendering showing long tubular forms of mitochondria. Approach to determine mitochondrial length (red) and variable shapes. To perform more accurate length measurement, mitochondria were segmented by drawing a series of connected spheres centered along the length of each mitochondrion using IMOD open contour.

Supplemental Movie 2. Rotating view of the final 3D images of *Apoa1bp*$^{-/-}$ Müller glia mitochondria. Surface rendering showing smaller, round forms of mitochondria. Approach to determine mitochondrial length (red) and variable shapes. To perform more accurate length measurement, mitochondria were segmented by drawing a series of connected spheres centered along the length of each mitochondrion using IMOD open contour.

Supplemental Movie 3. Rotating view of the final 3D images of WT RGC soma. Surface rendering of SBEM sub-volume showing cytoplasmic membrane (green), neurites (green), nucleus (blue) long tubular form (yellow) and branched mitochondria (red) in the WT RGC.

Supplemental Movie 4. Rotating view of the final 3D images of *Apoa1bp*$^{-/-}$ RGC soma. Surface rendering showing the cytoplasmic membrane, nucleus, dendrites and axons, and smaller round form (yellow) and branched (red) mitochondria in the *Apoa1bp*$^{-/-}$ RGC.

Supplemental Movie 5. Rotating view of the final 3D images of WT RGC mitochondrion. Surface rendering of the segmented volume emphasizes the density of the cristae (shades of brown). The mitochondrial outer membrane is shown in translucent maroon.

Supplemental Movie 6. Rotating view of the final 3D images of *Apoa1bp*$^{-/-}$ RGC mitochondrion. Surface rendering of the segmented volume emphasizes the less-dense cristae packing (shades of brown) and the 3 protuberances (black) that occupy part of the volume that would normally have been occupied by cristae.